# Investigation of magnetic field enriched surface enhanced resonance Raman scattering performance using Fe3O4@Ag nanoparticles for malaria diagnosis

Yuen, Clement; Liu, Quan

2014

Yuen, C., & Liu, Q. (2014). Investigation of magnetic field enriched surface enhanced resonance Raman scattering performance using Fe3O4@Ag nanoparticles for malaria diagnosis. SPIE Proceedings, 8955, 895516-.

https://hdl.handle.net/10356/103910

https://doi.org/10.1117/12.2038870

# Investigation of Magnetic Field enriched Surface Enhanced Resonance Raman Scattering Performance Using $Fe_3O_4$@Ag Nanoparticles for Malaria Diagnosis

Clement Yuen, Quan Liu*
Division of Bioengineering, School of Chemical and Biomedical Engineering, Nanyang Technological University, Singapore 637457

## ABSTRACT

Recently, we have demonstrated the magnetic field-enriched surface-enhanced resonance Raman spectroscopy (SERRS) of $\beta$-hematin by using nanoparticles with iron oxide core and silver shell ($Fe_3O_4$@Ag) for the potential application in the early malaria diagnosis. In this study, we investigate the dependence of the magnetic field-enriched SERRS performance of $\beta$-hematin on the different core and shell sizes of the $Fe_3O_4$@Ag nanoparticles. We note that the core and shell parameters are critical in the realization of the optimal magnetic field-enrich SERRS $\beta$-hematin signal. These results are consistent with our simulations that will guide the optimization of the magnetic SERRS performance for the potential early diagnosis in the malaria disease.

**Keywords:** Raman, surface enhanced Raman scattering (SERS), hemozoin, resonance Raman, hematin, malaria, discrete dipole approximation (DDA)

## 1. INTRODUCTION

We have previously demonstrated the development of magnetic field-enriched surface enhanced resonance Raman spectroscopy (SERRS) for early malaria diagnosis.[1] This magnetic field-enriched SERRS strategy dramatically enhanced the Raman spectra of $\beta$-hematin, which is equivalent to hemozoin (a malaria biomarker generated by malaria parasites) in Raman features, by using the nanoparticles with iron oxide core and silver shell ($Fe_3O_4$@Ag) enable SERRS. Although the plasmonic properties related to the different core and shell sizes of other types of nanoparticles have been examined in the literature,[2] the modified SERRS performance of these nanoparticles under an external magnetic field has never been evaluated before. Moreover, the paramagnetic $\beta$-hematin crystal under investigation in this strategy is much larger than the commonly used test molecules in surface-enhanced Raman spectroscopy such as Rhodamine 6G that are non-magnetic, which further complicate the optimization of nanoparticles for SERRS.

In this work, we investigate the dependence of magnetic field enriched SERRS performance of $\beta$-hematin on the core and shell sizes of $Fe_3O_4$@Ag nanoparticles. We note that Raman enhancement is improved in $Fe_3O_4$@Ag with a larger $Fe_3O_4$ core and a thicker Ag shell in the absence of a magnetic field. On the contrary, in the presence of an external magnetic field, $Fe_3O_4$@Ag with a smaller $Fe_3O_4$ core and a thinner Ag shell lead to the formation of more aggregates and hot spots that render a stronger Raman enhancement. These results are consistent with our simulations that will guide the optimization of magnetic SERRS for early malaria diagnosis.

## 2. MATERIALS AND METHODS

### 2.1 Core-shell $Fe_3O_4$@Ag nanoparticles synthesis

A coprecipitation method was used to fabricate the $Fe_3O_4$ nanoparticles.[3] NaOH at concentration of 4M was added drop-wise to the dissolved mixture of $FeCl_2 \cdot 4H_2O$ and $FeCl_3 \cdot 6H_2O$ at concentrations of 0.168 M and 0.333 M, respectively, at 60°C under vigorous mixing. The introduction of NaOH was ceased at pH values of 11, 13, and 14 to create different sizes of $Fe_3O_4$, followed with another 1-hour heating at 70°C under stirring.

*quanliu@ntu.edu.sg; phone: (65) 6316-8748; fax: (65) 6791-1761; http://www.ntu.edu.sg/home/quanliu/

Colloidal Nanoparticles for Biomedical Applications IX, edited by Wolfgang J. Parak, Marek Osinski, Kenji I. Yamamoto, Proc. of SPIE Vol. 8955, 895516 · © 2014 SPIE
CCC code: 1605-7422/14/$18 · doi: 10.1117/12.2038870

After cooled to room temperature, the nanoparticles were washed with deionized water after segregated from the mixture by using magnet. Next, 0.15 g of polyacrylic acid in 80 ml of ethanol was used to graft the aforesaid $Fe_3O_4$ nanoparticles in 20 ml ethanol at a concentration of 16.2 mM. This mixture was sonicated for 15 min and then the $Fe_3O_4$ nanoparticles were isolated from the mixture by using a magnet. The isolated $Fe_3O_4$ nanoparticles were washed and re-dispersed in ethanol and deionized water at a concentration with volume percent ratio of 80.6:19.4%. A seed-growth reduction method was used to fabricate Ag shell. In order to synthesize Ag shells of different thicknesses, we performed the followings in an ultrasonic bath to the aforesaid $Fe_3O_4$ nanoparticles suspension:

Set 1. Drop-wise $AgNO_3$ at concentration of 2.8 mM was added and mixed for 30 min, followed with the addition of 4.1 mM hydroxylamine hydrochloride, 8.1 mM NaOH, in triton X-100, ethanol, and deionized water at a concentration with volume percent ratio of 0.9:70.8:28.3 %;

Set 2. Additional 9.7 mM of $AgNO_3$ was added to set 1, in triton X-100, ethanol, and deionized water at a concentration with volume percent ratio 2:65.3:32.7%;

Set 3. 19.4 mM instead of 9.7 mM of $AgNO_3$ was used during the second-time $AgNO_3$ addition in the procedures as mentioned set 2;

Set 4. Same set 3 procedures were carried, except that an additional 9.7 mM was added into the mixture, prior to the introduction of triton X-100, ethanol, and deionized water.

Lastly, the $Fe_3O_4$@Ag nanoparticles were isolated by using a magnet and resuspended in 15 ml of methanol.

### 2.2 Raman measurements

A 785-nm laser was used to analyze all $\beta$ – hematin samples at an excitation power of 0.1 mW by using the above $Fe_3O_4$@Ag nanoparticles with a magnetic field of 0.198T and a magnetic field gradient of 26.6 $Tm^{-1}$ as stated in our other publication. An integration time of 10 s and a spectral resolution of 2 $cm^{-1}$ was employed for each acquired spectrum.

### 2.3 Discrete dipole approximation (DDA)

We calculated the electromagnetic field ($|E|^2$) distributions and the extinction efficiency ($Q_{ext}$) values of the $Fe_3O_4$@Ag nanoparticles with different core sizes and shell thickness using discrete dipole approximation (DDA) model.[4] We employed the DDA model since the technique is more efficient and flexible (comparing to the multiple multipole method and the finite difference time domain method).[5] The Amsterdam DDA code[6] was used for all the DDA calculations in this paper. All volumes under investigation were assumed to be comprised of only $Fe_3O_4$, Ag and $\beta$ – hematin only with electric constants[7, 8, 9] obtained from the literature. $Q_{ext}$ and $|E|^2$ of the $Fe_3O_4$@Ag nanoparticles with different core and shell parameters were calculated to evaluate against the experimental SERS performance, based on the fact that $Q_{ext}$ and $|E|^2$ are closely correlated to the SERS signals.

## 3. RESULTS

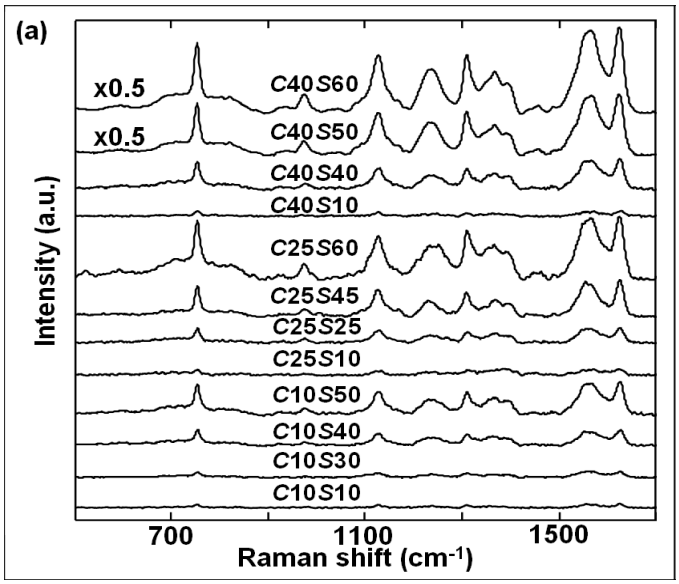

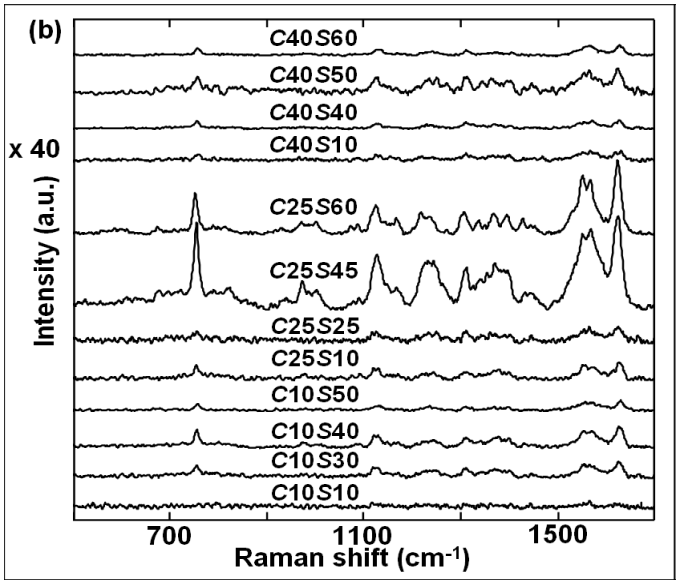


Figure 1. Experimental SERRS spectra of $\beta$ – hematin at (a) concentration 0.5 mM without magnetic-field enrichment and (b) concentration of 0.5 μM with magnetic-field enrichment by using $Fe_3O_4$@Ag nanoparticles of different core/shell parameters.

We characterized the SERRS performance of the fabricated $Fe_3O_4$@Ag nanoparticles with different dimension *C*40*S*60, *C*40*S*50, *C*40*S*40, *C*40*S*10, *C*25*S*60, *C*25*S*45, *C*25*S*25, *C*25*S*10, *C*10*S*50, *C*10*S*40, and *C*10*S*30, in which the first number indicates the $Fe_3O_4$ core radius and the second number gives the shell thickness. Figure 1 shows the SERRS spectra of $\beta$ – hematin (a) without and (b) with the influence of an external magnetic field by using different $Fe_3O_4$@Ag nanoparticles. Prominent Raman peaks were observed at 754, 1120, 1570, and 1628 $cm^{-1}$, which correspond to $\nu_{15}$ ($D_{4h}$ notation system for resonance Raman peaks studies on myoglobin),[21] $\nu_{22}$, $\nu_2$, and $\nu_{10}$, respectively. We note that the SERRS performance trend [Figure 1(a)], which has a greater SERRS signal with an increase in the core size and shell thickness in the $Fe_3O_4$@Ag nanoparticles, is dissimilar from that with the magnetic field enrichment [Figure 1(b)].

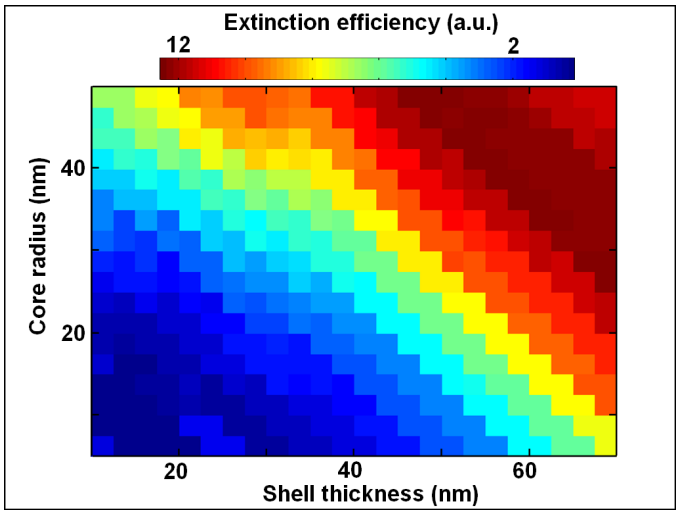


Figure 2. Calculated extinction efficiencies of $Fe_3O_4$@Ag nanoparticles with $Fe_3O_4$ core radius ranging from 5 nm to 50 nm and Ag shell thickness ranging from 10 nm to 70 nm using the DDA model at unpolarized 633-nm wavelength excitation.

We first employ DDA to calculate the extinction efficiency ($Q_{ext}$) of $Fe_3O_4$@Ag nanoparticles with $Fe_3O_4$ core radius ranging from 5 nm to 50 nm and Ag shell thickness ranging from 10 nm to 70 nm (Figure 2) since SERS intensities and the extinction efficiencies are related to the induced electromagnetic field, which is also applicable to other[2] plasmonic structures. The overall trend of the graph shows that $Q_{ext}$ value increases with the increase in the core radius and the shell thickness. This observation is consistent with $\beta$ – hematin SERRS in the case of without magnetic enrichment [Figure 1(a)]. The extinction efficiencies can predict the enhancement trends in the case of without an external magnetic field. In contrast, $\beta$ – hematin SERRS in the case of magnetic-field enrichment [Figure 1(b)] gives a different trend.

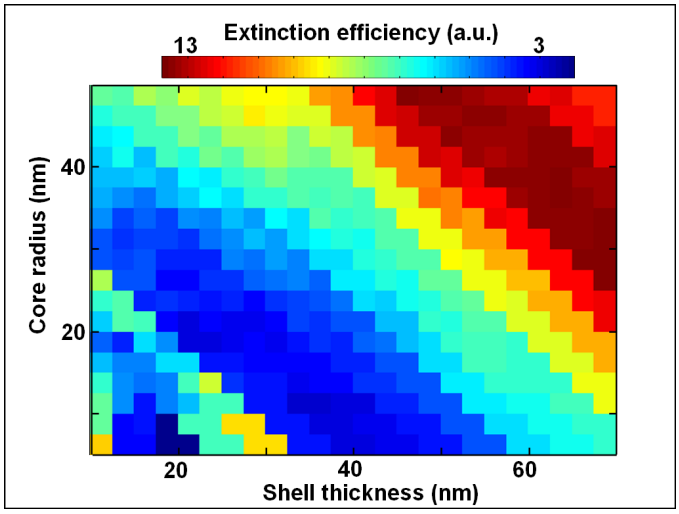


Figure 3. Extinction efficiencies of $Fe_3O_4$@Ag nanoparticles in dimer configuration with $Fe_3O_4$ core radius ranging from 5 nm to 50 nm and Ag shell thickness ranging from 10 nm to 70 nm at unpolarized 633-nm wavelength excitation.

One of the possible factors that modify the SERRS trends in the magnetic field-enriched SERRS performance could be attributed to aggregation of $Fe_3O_4$@Ag nanoparticles and $\beta$ – hematin. As for example, the extinction efficiency of the $Fe_3O_4$@Ag dimer (Figure 3) is different from a single $Fe_3O_4$@Ag nanoparticle (Figure 2). This further augmentation effect is noted even if the $Fe_3O_4$@Ag nanoparticles are separated from each other by a $\beta$ – hematin crystal of 40 nm (Figure 4). More details of this study can be found in our paper.[3]

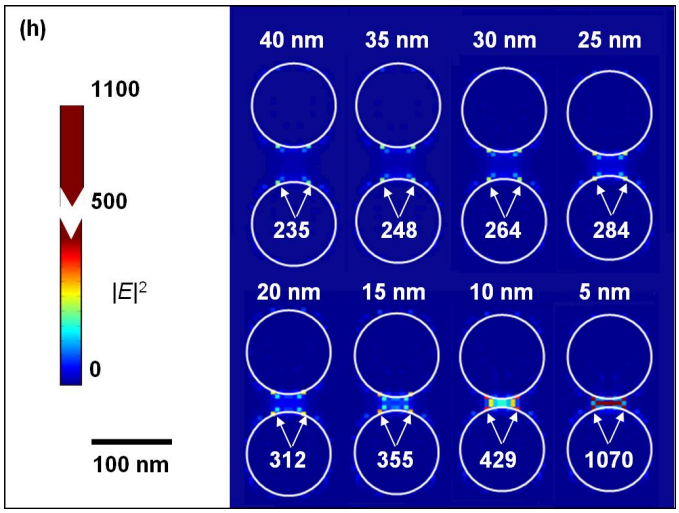


Figure 4. $|E|^2$ field distribution for two $Fe_3O_4$@Ag ($C25S25$) with a gap excited by vertically polarized 633-nm excitation, ranging from 5 nm to 40 nm, using the refractive index of $\beta$ – hematin for the surrounding medium. White circles demarcates locations of nanoparticles and number inside indicates the maximum $|E|^2$ intensity.

## 4. CONCLUSIONS

In conclusion, we have investigated theoretically and experimentally the magnetic field enriched SERRS phenomenon of $\beta$ – hematin by using $Fe_3O_4$@Ag with different core sizes and shell thicknesses. These results show that the magnetic field enriched SERRS by using $Fe_3O_4$@Ag shows great potential for early malaria diagnosis.

## ACKNOWLEDGEMENTS

The authors would like to acknowledge funding from the Lee Kuan Yew (LKY) start-up grant, the LKY research fellowship and the New Investigator Grant (Project No. NMRC/NIG/1044/2011) of National Medical Research Council (NMRC) in Singapore.

## REFERENCES

[1] Yuen, C. and Liu, Q., "Magnetic field enriched surface enhanced resonance Raman spectroscopy for early malaria diagnosis," J. Biomed. Opt. 17(1) 017005 (2012).

[2] Raschke, G., Brogl, S., Susha, A. S., Rogach, A. L., Klar, T. A., Feldmann, J., Fieres, B., Petkov, N., Bein, T., Nichtl, A. and Kurzinger, K., "Gold nanoshells improve single nanoparticle molecular sensors," Nano Lett. 4(10) 1853-1857 (2004).

[3] Yuen, C. and Liu, Q., "Optimization of $Fe_3O_4$@Ag nanoshells in magnetic field-enriched surface-enhanced resonance Raman scattering for malaria diagnosis," Analyst 138(21) 6494-6500 (2013).

[4] Yuen, C., Zheng, W. and Huang, Z., "Optimization of extinction efficiency of gold-coated polystyrene bead substrates improves surface-enhanced Raman scattering effects by post-growth microwave heating treatment," J. Raman Spectrosc. [41(4) 374-380 (2010).

[5] Yuen, C. and Liu, Q., "Towards in vivo intradermal surface enhanced Raman scattering (SERS) measurements: silver coated microneedle based SERS probe," J. Biophoton. 2013. DOI: 10.1002/jbio.201300006.

[6] Yurkin, M. A., and Hoekstra, A. G., "The discrete-dipole-approximation code ADDA: capabilities and known limitations," J. Quant. Spectrosc. Radiat. 112(13) 2234-2247 (2011).

[7] Johnson, P. B., and Christy, R. W., "Optical constants of the noble metals," Phys. Rev. B 6(12) 4370-4379 (1972).

[8] Schlegel, A., Alvarado, S. F. and Wachter, P., "Optical properties of magnetite ($Fe_3O_4$)," J. Phys. C 12(6) 1157-1164 (1979).

[9] Serebrennikova, Y. M., Patel, J. and Garcia-Rubio, L. H., "Interpretation of the ultraviolet-visible spectra of malaria parasite Plasmodium falciparum," Appl. Opt. 49(2) 180-188 (2010).